

Time-intensity curve in the abdominal aorta on dynamic contrast-enhanced MRI with high temporal and spatial resolution: Gd-EOB-DTPA versus Gd-DTPA in vivo

Yasunari Fujinaga · Hitoshi Ueda · Yoshihiro Kitou ·
Yoshinori Tsukahara · Yukiko Sugiyama ·
Masumi Kadoya

Received: 10 July 2012 / Accepted: 1 November 2012 / Published online: 20 November 2012
© Japan Radiological Society 2012

Abstract

Purpose To evaluate the difference in the time-intensity curves (TICs) of the abdominal aorta on dynamic contrast-enhanced MRI (DCE-MRI) between Gd-DTPA and Gd-EOB-DTPA.

Materials and methods Ten healthy volunteers underwent DCE-MRI three times with the following protocol: group A, Gd-DTPA at an injection rate of 3 ml/s; group B, Gd-EOB-DTPA, 3 ml/s; group C, Gd-EOB-DTPA, 1.5 ml/s. Signal intensities (SIs) of the abdominal aorta were measured, and the contrast enhancement ratio (CER) was calculated. Time-to-CER curves were compared among the three groups. The differences in maximum CER (CER_{max}) and time-to-peak of CER were analyzed.

Results The time-to-CER curve showed a double peak pattern in group A and single-peak pattern in groups B and C. The mean time between the first and the second peak was 6.2 s. The mean CER_{max} of each group was 4.50, 4.52 and 4.27, respectively. In group A, B and C, the mean time-to-peak was 14.6, 10.6 and 12.6 s, respectively. There was a significant difference between group A and B ($P < 0.01$).

Conclusion To set up the optimal protocol for abdominal DCE-MRI, it should be noted that TIC in the Gd-DTPA and Gd-EOB-DTPA group showed different patterns, and a slower injection rate showed a less abrupt SI change in the Gd-EOB-DTPA group than in the Gd-DTPA group.

Keywords Magnetic resonance imaging · Time-intensity curve · Gd-DTPA · Gd-EOB-DTPA · Ringing artifact

Introduction

Gadolinium ethoxybenzyl diethylenetriamine pentaacetic acid (gadoteric acid, Gd-EOB-DTPA; Primovist, Bayer Schering Pharma, Berlin, Germany) is a hepatocyte-specific contrast agent [1, 2] that has been used worldwide for abdominal contrast-enhanced MRI. The hepatobiliary phase of Gd-EOB-DTPA-enhanced MRI shows improved lesion detectability [3–7]. In addition, lesion vascularity can be assessed by dynamic contrast-enhanced MRI (DCE-MRI) using Gd-EOB-DTPA as well as an extracellular contrast agent because Gd-EOB-DTPA distributes into the extracellular fluid space just after injection and shows a T1-shortening effect.

There is controversy about the contrast effect of DCE-MRI using Gd-EOB-DTPA because its recommended amount and molar concentration are a half and a quarter of the extracellular contrast agent, respectively. Some authors compared the enhancement effect between Gd-EOB-DTPA and an extracellular agent, e.g., gadolinium diethylenetriamine pentaacetic acid (Gd-DTPA; Magnevist, Bayer Schering Pharma), and two groups reported that the contrast effect during arterial enhancement between the two was comparable [8, 9], while another group reported that the contrast effect with Gd-EOB-DTPA was lower than

This study received the Certificate for the Best Poster at the 3rd Asian Congress of Abdominal Radiology (ACAR) meeting in Beijing (2011).

Y. Fujinaga (✉) · Y. Tsukahara · Y. Sugiyama · M. Kadoya
Department of Radiology, Shinshu University School
of Medicine, 3-1-1 Asahi, Matsumoto 390-8621, Japan
e-mail: fujinaga@shinshu-u.ac.jp

H. Ueda · Y. Kitou
Radiology Division of Shinshu University Hospital,
3-1-1 Asahi, Matsumoto 390-8621, Japan

that with Gd-DTPA [10]. To compare the contrast effect of these contrast agents, it is important to clarify the difference of their time-intensity curves (TICs).

On the other hand, Svensson et al. [11] reported that a small variation in bolus timing could yield large variations in the appearance of the vessel if the center of the k-space is sampled during a rapid contrast-medium concentration variation. The ringing artifact was attributed to abrupt signal change in the abdominal aorta and was sometimes seen on DCE-MRI using Gd-EOB-DTPA [12]. Motosugi et al. [13] reported that the dilution method of Gd-EOB-DTPA-enhanced dynamic MRI provided better image quality in comparison with non-dilution methods. It is important to validate TIC to set up optimal sequence parameter, such as the scan time and center of k-space. But we cannot evaluate the TIC with the dilution method because of off-label use of Gd-EOB-DTPA. Tamada et al. [14] reported that the image quality of DCE-MRI using Gd-EOB-DTPA at the injection rate of 1 ml/s was better than that using the dilution method. Therefore, we considered that we should know the TIC of DCE-MRI also with low injection speed instead of the dilution method.

Time-resolved angiography with interleaved stochastic trajectory (TWIST) sequences is one of the view-sharing 3D sequences and provides good MR images with excellent temporal resolution and high image quality without prolongation of the acquisition time. Its sequence is available for not only MR angiography, but also perfusion analysis [15]. In addition, TIC in the abdominal aorta of small animals at DCE-MRI was analyzed by this sequence [16]. Hence, the TWIST sequence has the potential to provide excellent TIC in the abdominal aorta of humans.

There are no articles comparing detailed TICs of DCE-MRI using Gd-EOB-DTPA and extracellular agents in humans. The purpose of this study was to evaluate the difference in the TIC and contrast-enhanced effect in the abdominal aorta between Gd-EOB-DTPA-enhanced dynamic MRI and extracellular-agent-enhanced dynamic MRI, and between Gd-EOB-DTPA-enhanced dynamic MRI with conventional injection speed and low injection speed, and to obtain useful information for setting up optimal Gd-EOB-DTPA-enhanced DCE-MRI using the TWIST sequence.

Materials and methods

Volunteers

Ten healthy volunteers were evaluated with DCE-MRI. The volunteers, who had no history of digestive, circulatory or urologic disease, were recruited in our hospital and consisted of nine men and one woman who ranged in age from 23 to 54 years (mean age 33.7 years).

This study was approved by the institutional review board of our institution, and each volunteer gave written informed consent to participate.

MR imaging

All MR images were obtained with a 3-T MR unit (Magnetom Trio, Siemens Medical Systems, Erlangen, Germany) using a standard body array coil provided by the manufacturer. DCE-MRI was performed using the TWIST sequence. Imaging parameters were as follows: TR, 3.56 ms; TE, 1.04 ms; flip angle, 10°; bandwidth, 1,030 Hz/pixel; field of view (FOV), 450 × 450 mm; matrix, 512 × 512; number of partitions, 40; temporal resolution, 2 s. In all sequences, we used a 1-2-1 binominal radiofrequency (RF) excitation pulse to avoid paradoxical negative enhancement and generalized autocalibrating partially parallel acquisition (GRAPPA) [17] with an acceleration factor of 2 to optimize sequences.

The TWIST sequence uses two regions [inner (A) and outer (B)] of k-space (Fig. 1). First, full sampling of A and B was performed, followed by consecutive sampling of each region. The TWIST sequence is based on undersampling of both regions, and the density of each area can be set at any level. In addition, the percentage of A and B can be selected. MR images were reconstructed from adjacent data sets (Fig. 2). We used the value of A:B = 1:1 (i.e., each region was 50 % of the total k-space) and density of A = 25 % and B = 10 %.

Eighteen coronal image sets were acquired by Dynamic MRI with 39 s breath-hold (time resolution of the first scan was 6 s and that of following 17 scans was 2) in one examination.

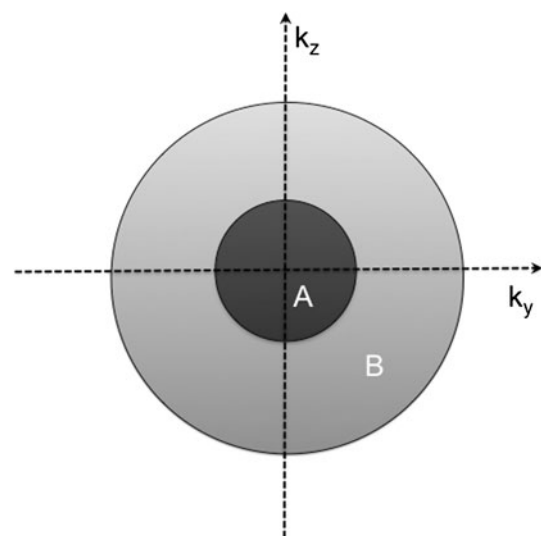
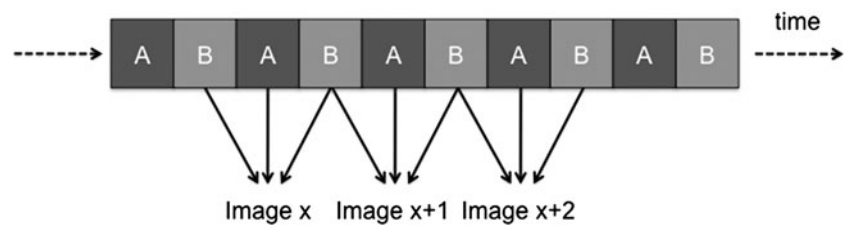


Fig. 1 The property of k-space. The TWIST sequence uses A and B with two different sampling properties

Fig. 2 Reconstruction of MR images. The TWIST sequence uses adjacent data sets to reconstruct the MR images



Contrast dose and injection rate

Two contrast agents, Gd-EOB-DTPA and an extracellular agent, such as gadolinium diethylenetriamine pentaacetic acid (Gd-DTPA; Magnevist, Bayer Schering Pharma), were used at standard doses (Gd-EOB-DTPA, 0.025 mmol/kg body weight; Gd-DTPA, 0.1 mmol/kg body weight).

Contrast agent was injected through a 21-gauge catheter placed in the cubital vein followed by 40 ml of 0.9 % saline injection at the same rate as the contrast agent. Injection of contrast agent and saline was performed with an MRI-compatible injector. In this study, we prepared three types of agent injection methods and classified them into three groups as follows: group A, injection of Gd-DTPA at a flow rate of 3 ml/s; group B, injection of Gd-EOB-DTPA at a flow rate of 3 ml/s; group C, injection of Gd-EOB-DTPA at a flow rate of 1.5 ml/s.

Dynamic MRI

All volunteers underwent dynamic MRI three times using each of the injection types, i.e., three post-contrast data sets were acquired in each patient. DCE-MRI of group B and C was performed about 1 week after that of group A and B, respectively.

Contrast agent injection was started few seconds after commencing the MR scanning because we had to obtain both precontrast images and postcontrast images to analyze the TIC.

MR imaging analysis

MR images were analyzed using regions of interest (ROIs) with a commercial software package, EV Insite (PSP Corp., Tokyo, Japan). Oval ROIs (121.4–175.9 mm²; mean 150.8 mm²) were set in the abdominal aorta at the level of the celiac artery by one abdominal radiologist (YF with 17 years of experience), and the signal intensity (SI) of the ROIs was measured in each image. This procedure was performed again 1 month after first measurement by the same radiologist. We calculated the mean of the SI in each image.

To calibrate the TIC, we considered that the phase was 0 s when the contrast agent arrived at the pulmonary artery (Fig. 3). At this time, the contrast agent had not yet arrived at the abdominal aorta. Because our protocol included the

parallel imaging method and it was ineligible to analyze the signal-to-noise ratio, we calculated the contrast-enhancement ratio (CER) using the following equation: $CER = (SI - SI_0)/SI_0$ (SI_0 , SI at 0 s).

CER was used for analysis of the time-to-CER curve as a TIC, maximum CER (CER_{max}) and time-to-peak.

Statistical analysis

Kruskal-Wallis test was used to compare the differences in time-to-peak and CER_{max} among each injection type. Mann-Whitney *U* test was also used to compare two data sets in one group. All statistical tests were two tailed, and differences with $P < 0.05$ were regarded as statistically significant. The statistical tests were performed using software (Prism, version 5; GraphPad Software, San Diego, CA, USA).

Results

The time-to-CER curve was different for each injection type (Fig. 4). Regarding group A, the time-to-CER curve showed a double-peak pattern in all volunteers, with the CER of the first peak lower than that of the second peak in 8 of 10. CER of the first peak (4.46 ± 1.04) was not significantly different from that of the second peak (4.519 ± 1.11) according to the Mann-Whitney *U* test ($P = 0.733$). The mean time between the first and the second peak was 6.2 ± 1.99 s. There was no volunteer whose time-to-CER curve showed the double-peak pattern in group B or C.

The mean CER_{max} and standard deviation of each group were 4.50 ± 1.06 , 4.52 ± 0.93 and 4.27 ± 0.59 , respectively (Fig. 5). There was no significant difference between any of the groups ($P = 0.598$).

The mean time-to-peak and standard deviation of group A, B and C were 14.6 ± 2.12 , 10.6 ± 1.90 and 12.6 ± 1.65 s, respectively (Fig. 6). There was a significant difference between group A and B ($P < 0.01$).

Discussion

Zech et al. [8] performed Gd-EOB-DTPA- and Gd-DTPA-enhanced MRI with two kinds of injection rate (1 and 2 ml/s)

Fig. 3 Calibration of the time-intensity curve. Sequential MR images show the contrast agent arriving at the pulmonary artery on image 8 (white arrows). We consider this image as time zero. The contrast agent arrives at the abdominal aorta on image 11 (white open arrow), i.e., at 6 s, because the time resolution of each image was 2 s

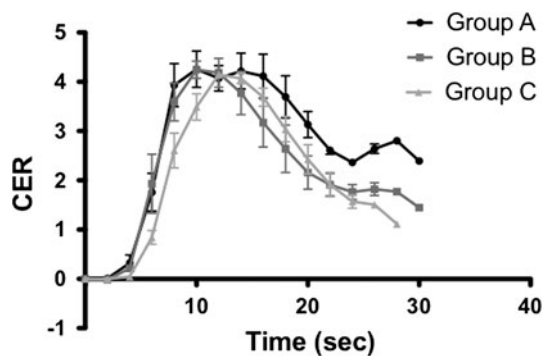
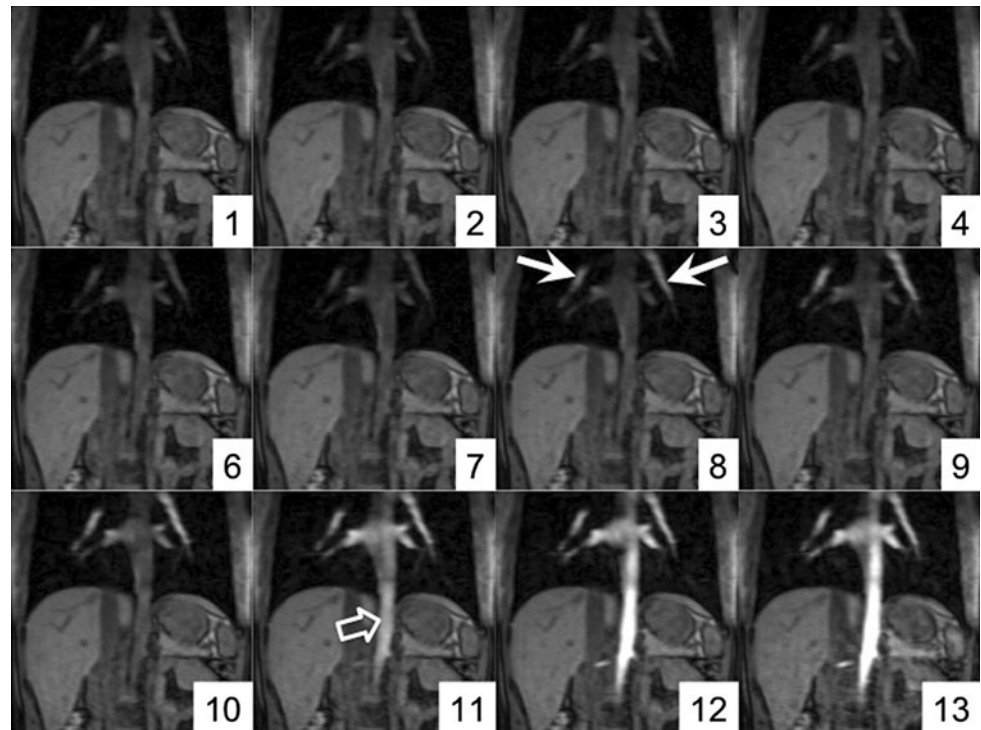


Fig. 4 Time-to-CER curve. Double-peak pattern is seen in group A, and there is a more abrupt change of the time-to-CER curve in group B than in group C. CER contrast enhancement ratio

and two kinds of Gd-EOB-DTPA dose (standard dose and double dose) in an animal model (pigs). In this article, double-dose Gd-EOB-DTPA at a lower-flow rate of 1 ml/s showed the highest signal-to-noise ratio (SNR) and standard dose Gd-EOB-DTPA at the rate of 2 ml/s showed the lowest SNR in the abdominal aorta. These results were different from ours. There was a critical problem in their study because the time resolution was 5 s although the TIC around the peak was very steep. In addition, the blood circulation in pigs is not the same as that in humans.

In this study, we analyzed TICs focusing on the aorta with excellent time resolution of 2 s and found that the TIC of an extracellular agent shows a double-peak pattern in the abdominal aorta. We did not measure other vessels (portal vein and hepatic vein) and liver parenchyma because the

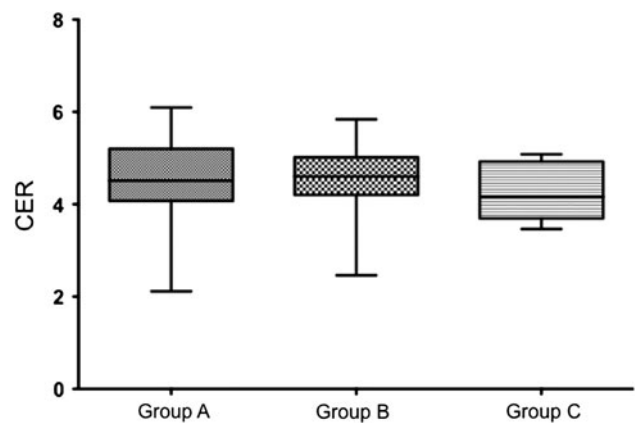


Fig. 5 Maximum contrast-enhancement ratio (CER_{max}) of the three groups. Box-and-whisker plots show median (middle line of box), quartiles (top and bottom lines of box), upper extreme value (upper whisker) and lower extreme value (lower whisker) for CER_{max}. There was no significant difference between any of the groups by Kruskal-Wallis test ($P = 0.598$)

TIC in the aorta is most important for establishing an optimal DCE-MRI method. We considered that in group A the second peak, which was higher than the first peak in most subjects and appeared to be about 6 s after the first peak, did not correspond to the second-pass peak, because the second-pass peak was generally lower than the first-pass peak and was observed about 20 s after the first-pass peak [18–20]. Although the density of Gd-DTPA was proportional to its concentration on CT, the signal intensity of Gd-DTPA was not proportional to its concentration on

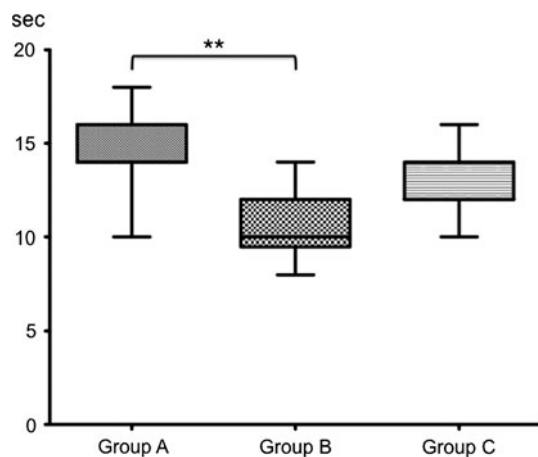


Fig. 6 Time-to-peak of the three groups. *Box-and-whisker plots* show median (*middle line of box*), quartiles (*top and bottom lines of box*), upper extreme value (*upper whisker*) and lower extreme value (*lower whisker*) for time to peak. Median and lower quartiles overlap in group A and C. There was a significant difference between group A and B by Kruskal–Wallis test. ****** $P < 0.01$

MRI [21], because extracellularly distributed Gd-DTPA on MRI showed T2* effects [19]. Therefore, we considered that the signal intensity was reduced at the peak Gd-DTPA concentration because of increased T2* effects, and a double-peak pattern was formed. In addition, the T2* effect on 3D-gradient echo (GRE) images was stronger than that on 2D-GRE images [22]. It might be one of the factors of the double peak formation because we used the TWIST sequence, which was one of the 3D-GRE sequences. On the other hand, the TIC of Gd-EOB-DTPA showed a single-peak pattern with each injection speed. This phenomenon means that the T2* effects of Gd-EOB-DTPA at the peak concentration were less than those of Gd-DTPA.

There was no significant difference in the mean CER_{max} between any of the groups. We could explain that CER_{max} peaked at about 4.5 because of increased T2* effects. When DCE-MRI was performed using Gd-DTPA with an injection rate of 3 ml/s, the maximum concentration of the aorta was 4.9–5 mM [19, 23]. When the concentration of the Gd-DTPA was over 4 mM, the relation between the MR signal and Gd-DTPA concentration did not show a linear relation, and the real signal intensity was lower than the theoretical one [21]. The mean CER_{max} in group C was slightly lower than that in group A and B because the peak Gd-DTPA concentration at the injection rate of 3 ml/s was higher than that at the injection rate of 1.5 ml/s, and the signal intensity showed a concentration-dependent increase until saturation was reached [22, 23].

In group A, CER at the second peak might be nearer than that at the first peak because of the following factors: (1) time resolution was 2 s in this study, (2) CER was rapidly increased until the time of the first peak and

gradually decreased after the second peak, (3) the T2* effect appeared suddenly and strongly after the first peak and disappeared gradually at the second peak. In the previous report, signal changes in the aorta also showed a double-peak pattern, and the signal intensity of the first peak was lower than that of the second peak [19].

Truncation or Gibbs artifact, the so-called as ringing artifact, consists of bright or dark lines that are seen parallel to edges of abrupt intensity change [11, 24]. It is sometimes seen on DCE-MRI because the abrupt flow of the contrast agent breaks the k-space homogeneity [11, 13]. Tanimoto et al. reported that the ringing artifact could be reduced by selecting a shorter scanning time because the signal intensity change during a shorter acquisition time was smaller than that during a longer one [25]. The trade-off for the shorter scanning time is decreasing image quality. On the other hand, the signal change between the double peaks in group A was gradual. It is an advantage for reducing the ringing artifact of MR images at the arterial phase. In addition, it may allow longer scanning times for obtaining high-quality images because gradual signal change between two peaks lasted for over 6 s.

As for the comparison between group B and C, i.e., in the Gd-EOB-DTPA group, the time-to-peak of group B was shorter and the time-to-CER curve was steeper than that of group C. This fact suggests that MR images with an injection rate of 3 ml/s might be more affected by ringing artifacts caused by the abrupt intensity change than that with 1.5 ml/s. On the other hand, there was no significant CER_{max} difference between them. Therefore, DCI-MRI with a slow injection rate may have an advantage for a good-quality image because of having an equal contrast enhancement effect and a minor effect of ringing artifacts in comparison to that with a rapid injection rate.

This study has some limitations. First, only a small number of volunteers were used. We considered that it would be difficult to analyze many clinical patients because the MRI protocol in this study was ineligible for clinical diagnosis, and it would be unethical to enroll many volunteers. To reduce the effect of this small number, we performed DCE-MRI three times in each volunteer. Second, the age, gender, weight and height of the volunteers were variable, and there was some selection bias. But this problem was unavoidable in this study design. Third, the size of the ROIs set on the aorta was variable. Mendičovszky et al. [20] reported that the size of the ROI significantly affected the signal intensity. In this study, this problem was minor because the square of ROI in each group was not significantly different ($P = 0.355$).

In conclusion, the TIC in group A (Gd-DTPA, 3 ml/s), which was shown as a double-peak pattern, was different from that of group B (Gd-EOB-DTPA, 3 ml/s) and group C (Gd-EOB-DTPA, 1.5 ml/s), which was shown as a single-

peak pattern. In the Gd-DTPA group, the slower injection rate showed a less abrupt change. In consideration of the theory of truncation artifacts, the differences in the TIC potentially influence the degree of the ringing artifact. Radiologists should know the TIC differences in each group to set up an optimal scan protocol.

Acknowledgments We thank Kastuya Maruyama, Siemens Japan K.K., for comments on the MR sequences. This study was supported in part by the Ministry of Health, Labour and Welfare, research on hepatitis, and Japanese Health and Labor Sciences research grants for the development of early detection systems for liver cancer using molecular markers and diagnostic imagings.

References

- Schuhmann-Giampieri G, Schmitt-Willich H, Press WR, Negishi C, Weinmann HJ, Speck U. Preclinical evaluation of Gd-EOB-DTPA as a contrast agent in MR imaging of the hepatobiliary system. *Radiology*. 1992;183:59–64.
- Reimer P, Rummeny EJ, Shamsi K, et al. Phase II clinical evaluation of Gd-EOB-DTPA: dose, safety aspects, and pulse sequence. *Radiology*. 1996;199:177–83.
- Huppertz A, Balzer T, Blakeborough A, et al. Improved detection of focal liver lesions at MR imaging: multicenter comparison of gadoxetic acid-enhanced MR images with intraoperative findings. *Radiology*. 2004;230:266–75.
- Bluemke DA, Sahani D, Amendola M, et al. Efficacy and safety of MR imaging with liver-specific contrast agent: US multicenter phase III study. *Radiology*. 2005;237:89–98.
- Hammerstingl R, Huppertz A, Breuer J, et al. Diagnostic efficacy of gadoxetic acid (Primovist)-enhanced MRI and spiral CT for a therapeutic strategy: comparison with intraoperative and histopathologic findings in focal liver lesions. *Eur Radiol*. 2008;18:457–67.
- Petersein J, Spinazzi A, Giovagnoni A, et al. Focal liver lesions: evaluation of the efficacy of gadobenate dimeglumine in MR imaging—a multicenter phase III clinical study. *Radiology*. 2000;215:727–36.
- Oudkerk M, Torres CG, Song B, et al. Characterization of liver lesions with mangafodipir trisodium-enhanced MR imaging: multicenter study comparing MR and dual-phase spiral CT. *Radiology*. 2002;223:517–24.
- Zech CJ, Vos B, Nordell A, et al. Vascular enhancement in early dynamic liver MR imaging in an animal model: comparison of two injection regimen and two different doses Gd-EOB-DTPA (gadoxetic acid) with standard Gd-DTPA. *Invest Radiol*. 2009;44:305–10.
- Kuhn JP, Hegenscheid K, Siegmund W, Froehlich CP, Hosten N, Puls R. Normal dynamic MRI enhancement patterns of the upper abdominal organs: gadoxetic acid compared with gadobutrol. *Am J Roentgenol*. 2009;193:1318–23.
- Tamada T, Ito K, Sone T, et al. Dynamic contrast-enhanced magnetic resonance imaging of abdominal solid organ and major vessel: comparison of enhancement effect between Gd-EOB-DTPA and Gd-DTPA. *J Magn Reson Imaging*. 2009;29:636–40.
- Svensson J, Petersson JS, Stahlberg F, Larsson EM, Leander P, Olsson LE. Image artifacts due to a time-varying contrast medium concentration in 3D contrast-enhanced MRA. *J Magn Reson Imaging*. 1999;10:919–28.
- Tanimoto A, Lee JM, Murakami T, Huppertz A, Kudo M, Grazioli L. Consensus report of the 2nd International Forum for Liver MRI. *Eur Radiol*. 2009;19(Suppl 5):S975–89.
- Motosugi U, Ichikawa T, Sou H, et al. Dilution method of gadolinium ethoxybenzyl diethylenetriaminepentaacetic acid (Gd-EOB-DTPA)-enhanced magnetic resonance imaging (MRI). *J Magn Reson Imaging*. 2009;30:849–54.
- Tamada T, Ito K, Yoshida K, et al. Comparison of three different injection methods for arterial phase of Gd-EOB-DTPA enhanced MR imaging of the liver. *Eur J Radiol*. 2011;80:e284–8.
- Bauman G, Scholz A, Rivoire J, et al. Lung ventilation- and perfusion-weighted Fourier decomposition magnetic resonance imaging: In vivo validation with hyperpolarized (3 He) and dynamic contrast-enhanced MRI. *Magn Reson Med*. 2012 (Epub ahead of print).
- Giesel FL, Runge V, Kirchin M, et al. Three-dimensional multiphase time-resolved low-dose contrast-enhanced magnetic resonance angiography using TWIST on a 32-channel coil at 3 T: a quantitative and qualitative comparison of a conventional gadolinium chelate with a high-relaxivity agent. *J Comput Assist Tomogr*. 2010;34:678–83.
- Griswold MA, Jakob PM, Heidemann RM, et al. Generalized autocalibrating partially parallel acquisitions (GRAPPA). *Magn Reson Med*. 2002;47:1202–10.
- Michoux N, Montet X, Pechere A, et al. Parametric and quantitative analysis of MR renographic curves for assessing the functional behaviour of the kidney. *Eur J Radiol*. 2005;54:124–35.
- de Bazelaire C, Rofsky NM, Duhamel G, et al. Combined T2* and T1 measurements for improved perfusion and permeability studies in high field using dynamic contrast enhancement. *Eur Radiol*. 2006;16:2083–91.
- Mendichovszky IA, Cutajar M, Gordon I. Reproducibility of the aortic input function (AIF) derived from dynamic contrast-enhanced magnetic resonance imaging (DCE-MRI) of the kidneys in a volunteer study. *Eur J Radiol*. 2009;71:576–81.
- Pudrzbach M, Risse F, Biederer J, et al. In vivo Gd-DTPA concentration for MR lung perfusion measurements: assessment with computed tomography in a porcine model. *Eur Radiol*. 2008;18:2102–7.
- Morita K, Namimoto T, Awai K, et al. Enhancement effects of hepatic dynamic MR imaging at 3.0 T and 1.5 T using gadoxetic acid in a phantom study: comparison with gadopentetate dimeglumine. *Magn Reson Med*. 2011;66:213–8.
- Ishida M, Sakuma H, Murashima S, et al. Absolute blood contrast concentration and blood signal saturation on myocardial perfusion MRI: estimation from CT data. *J Magn Reson Imaging*. 2009;29:205–10.
- Stadler A, Schima W, Ba-Ssalamah A, Kettenbach J, Eisenhuber E. Artifacts in body MR imaging: their appearance and how to eliminate them. *Eur Radiol*. 2007;17:1242–55.
- Tanimoto A, Higuchi N, Ueno A. Reduction of ringing artifacts in the arterial phase of gadoxetic acid-enhanced dynamic MR imaging. *Magn Reson Med Sci*. 2012;11:91–7.